Radiat Environ Biophys (2011) 50:371–381
DOI 10.1007/s00411-011-0360-2

ORIGINAL PAPER

# Chromosome aberration measurements in mitotic and $G_2$-PCC lymphocytes at the standard sampling time of 48 h underestimate the effectiveness of high-LET particles

**Ryonfa Lee · Elena Nasonova · Carola Hartel · Marco Durante · Sylvia Ritter**

Received: 29 October 2010 / Accepted: 20 March 2011 / Published online: 11 April 2011


**Abstract** The relationship between heavy-ion-induced cell cycle delay and the time-course of aberrations in first-cycle metaphases or prematurely condensed $G_2$-cells ($G_2$-PCC) was investigated. Lymphocytes of the same donor were irradiated with X-rays or various charged particles (carbon, iron, xenon, and chromium) covering an LET range of 2–3,160 keV/μm. Chromosome aberrations were measured in samples collected at 48, 60, 72, and 84 h postirradiation. Linear-quadratic functions were fitted to the data, and the fit parameters $\alpha$ and $\beta$ were determined. At any sampling time, $\alpha$ values derived from $G_2$-cells were higher than those from metaphases. The $\alpha$ value derived from metaphase analysis at 48 h increased with LET, reached a maximum around 155 keV/μm, and decreased with a further rise in LET. At the later time-points, higher $\alpha$ values were estimated for particles with LET $>$ 30 keV/μm. Estimates of $\alpha$ values from $G_2$-cells showed a similar LET dependence, yet the time-dependent increase was less pronounced. Altogether, our data demonstrate that heavily damaged lymphocytes suffer a prolonged $G_2$-arrest that is clearly LET dependent. For this very reason, the standard analysis of aberrations in metaphase cells 48 h postirradiation will considerably underestimate the effectiveness of high-LET radiation. Scoring of aberrations in $G_2$-PCC at 48 h as suggested by several authors will result in higher aberration yields. However, when particles with a very high-LET value (LET $>$ 150 keV/μm) are applied, still a fraction of multiple damaged cells escape detection by $G_2$-analysis 48 h postirradiation.

R. Lee · E. Nasonova · C. Hartel · M. Durante · S. Ritter (✉)
Biophysics Department, GSI Helmholtzzentrum für Schwerionenforschung, Planckstraße 1, 64291 Darmstadt, Germany
e-mail: s.ritter@gsi.de

E. Nasonova
Laboratory of Radiation Biology, Joint Institute for Nuclear Research, Joliot-Curie 6, 141980 Dubna, Moscow region, Russia

M. Durante
Department of Condensed Matter Physics, Technical University of Darmstadt, Hochschulstraße 6-8, 64289 Darmstadt, Germany

## Introduction

The measurement of chromosome aberrations in human peripheral blood lymphocytes at mitosis is a sensitive and frequently applied method to assess the individual dose following accidental, occupational, or medical exposure to ionizing radiation (IAEA 2001) and to estimate possible health risks (Bonassi et al. 2008). The technique has been widely applied over the last 50 years when physical dosimetry was not available or as an independent method to supplement physical measurements (e.g., see Lindholm et al. 1996; Sasaki et al. 2001; Wojcik et al. 2003). Likewise, in many studies, the metaphase assay has been used to estimate the relative biological effectiveness (RBE) of high-LET exposure (e.g., Testard et al. 1997; Bauchinger and Schmid 1998). According to the routinely applied protocol (IAEA 2001), a venipuncture blood sample is taken and the whole blood or isolated lymphocytes are cultured in vitro in medium supplemented with phytohemagglutinin (PHA), a mitogen that preferentially stimulates T-lymphocytes to enter the cell cycle. Lymphocytes are cultured for 48 h and during the last 2–3 h of incubation, colcemid is added to the cultures to achieve a high yield of first-cycle metaphases. Then, metaphase spreads are prepared, and chromosome aberrations are scored. For biological dosimetry, the measured aberration frequency is compared with a calibration dose–response curve

generated by the exposure of lymphocytes in vitro and cultured as described previously (IAEA 2001), while for the estimation of the RBE, the dose of the test radiation (e.g., heavy ions) and the reference radiation (e.g., X-rays) required for the induction of the same level of damage are compared.

In recent years, data accumulate showing that the analysis of chromosome aberrations in lymphocytes collected at the standard fixation time of 48 h underestimates the damage produced by high-LET radiation (Ritter and Durante 2010). The exposure of cells to high-LET radiation delays the cell cycle progression more than the exposure to low-LET radiation (Lucke-Huhle et al. 1979; Scholz et al. 1994; Ochab-Marcinek et al. 2009), and it has been recently demonstrated that the delay time is related to the number of aberrations carried by a cell (Gudowska-Nowak et al. 2005; Deperas-Standylo et al. 2010). For human lymphocytes, the delayed entry of heavily damaged cells into mitosis has been attributed to a prolonged $G_2$-arrest (Durante et al. 1999; George et al. 2001, 2003). Consequently, if high-LET-induced chromosome aberrations are only quantified at 48 h, heavily damaged and drastically delayed lymphocytes are excluded from the analysis (Anderson et al. 2000; George et al. 2001; Ritter et al. 2002; Nasonova and Ritter 2004; Lee et al. 2005, 2010). This might result in an underestimation of the RBE of heavy ions (Ritter et al. 1996; Anderson et al. 2000; Suzuki et al. 2000; Ritter et al. 2002; Nasonova and Ritter 2004) or the dose of a mixed radiation field as discussed by Durante et al. (1997). To gain a realistic estimate of the amount of damage produced by high-LET radiation within the entire cell population, the use of multiple sampling times that cover the complete time interval of the first mitosis together with a mathematical folding of the data has been suggested (Scholz et al. 1998). However, since heavy ion exposure may delay the progression of lymphocytes to mitosis for up to 50 h (e.g., Nasonova and Ritter 2004; Lee et al. 2010), this technique is too labor-intensive for routine applications.

Alternatively, as a fast and simple method to quantify chromosomal damage in cells that suffer a prolonged $G_2$-arrest and thus escape conventional metaphase analysis at 48 h, the chemically induced premature chromosome condensation (PCC) technique has been proposed (Durante et al. 1998; Kanda et al. 1999; Gotoh and Tanno 2005). As in the conventional metaphase assay, lymphocytes are stimulated to grow and cultured for 48 h. During the last 30 min to 1 h, calyculin A or okadaic acid is added to the cell culture medium inducing PCC predominantly in $G_2$-cells (see Gotoh and Durante 2006 and references therein). Then, aberrations are analyzed in $G_2$ or $G_2$/M-cells. Indeed, when chromosome aberrations were scored in prematurely condensed lymphocytes collected at 48 h after heavy ion exposure, higher aberration yields were obtained than for metaphases collected at the same time (Durante et al. 1999; Ritter et al. 2002; George et al. 2003; Nasonova and Ritter 2004; Lee et al. 2005). However, up to now, little is known about the LET dependence of the $G_2$-arrest in human lymphocytes, and it has not been experimentally demonstrated to what extent the drug-induced PCC assay at 48 h postirradiation accounts for high-LET-induced cell cycle delay of heavily damaged lymphocytes that prevents their entry into mitosis.

To clarify this point, we exposed lymphocytes to heavy ions and measured the aberration yields at several sampling times in both first-cycle $G_2$-PCC and first-cycle metaphase cells. Main emphasis was placed on the effects of C-ions and Fe-ions. A better knowledge of the cytogenetic effects of C-ions is required, since their application in cancer therapy is comparatively new (Tsujii et al. 2008; Fokas et al. 2009; Schulz-Ertner 2009; Durante and Loeffler 2010; Minohara et al. 2010 and references therein), and the induction of late effects such as secondary malignancies is of major concern especially for the treatment of young patients (Dickerman 2007; Combs et al. 2009; Merchant 2009). Likewise, for space radiation protection, more information is needed on the effects of high-Z and high-energy (HZE) particles such as Fe-ions that pose the highest health risk to astronauts (Cucinotta and Durante 2006; Durante and Cucinotta 2008).

## Materials and methods

### Cell culture and irradiation

For all experiments, peripheral blood was obtained from a nonsmoking female volunteer who gave informed consent, and the study was approved by the international advisory board at GSI. Immediately after blood collection into vacutainer cell preparation tubes (Beckton Dickinson, USA), lymphocytes were isolated by centrifugation. Cells were resuspended at a density of $4 \times 10^6$/ml in RPMI 1640 medium supplemented with 20% fetal calf serum, 2 mM L-glutamine, 100 U/ml penicillin, and 100 µg/ml streptomycin referred to as complete medium (Durante et al. 1998).

Lymphocytes were exposed to X-rays (250 kV, 16 mA, 1 mm Al + 1 mm Cu filtering) or charged particles with different energies at GSI (Darmstadt, Germany). Exposure to particles with energies $\geq$ 100 MeV/u was done at the heavy ion synchrotron SIS (Haberer et al. 1993), while the exposure to particles with an energy of 11.4 MeV/u was performed at the linear accelerator UNILAC (Kraft et al. 1980). All irradiations were done at room temperature, and control samples were sham-irradiated. For heavy ions, the irradiation time was in the range of 1–4 min depending on

**Table 1** Information on the radiations applied in this study and sampling times for the detection of chromosome aberrations

| Radiation type | $E_{prim}$ (MeV/u) | E (MeV/u) | LET (keV/μm) | $R_{max}$ (μm) | Range (mm) | Dose (Gy) | Fluence ($\times 10^6$/cm$^2$) | Sampling times (h) | |
|---|---|---|---|---|---|---|---|---|---|
| | | | | | | | | Metaphases | $G_2$-PCC |
| X-rays | | | 2 | | | 0.3, 0.6, 1, 2, 3, 4, 6 | | 48[d], 60[d], 72[d] | 48[d], 60, 72 |
| Monoenergetic particle beams | | | | | | | | | |
| Carbon | 400[a] | 396 | 11 | 1,300 | 266 | 1, 2, 4 | 57, 113, 227 | 48 | – |
| | 270[a] | 265 | 14 | 680 | 137 | 0.5, 1, 2, 4 | 23, 46, 93, 185 | 48, 72 | – |
| | 100[a] | 90 | 29 | 103 | 20 | 0.3, 0.6, 1, 2, 3, 4 | 6.5, 13, 22, 43, 65, 86 | 48, 60, 72 | 48, 60, 72 |
| | 11.4[b] | 9.5 | 175 | 2.3 | 0.39 | 1, 2, 4 | 3.6, 7.1, 14 | 48, 60, 72, 84 | 48, 60, 72, 84 |
| Iron | 1,000[a] | 990 | 155 | 6,200 | 258 | 1, 2.2, 3 | 4, 9, 12 | 48[e], 60[e], 72[e], 84[e] | 48[e], 60, 72 |
| | 200[a] | 177 | 335 | 330 | 16 | 0.5, 1.1, 2.2, 3.2, 4.3 | 1, 2, 4, 6, 8 | 48, 60, 72, 84 | 48, 60, 72 |
| | 200[c] | 115 | 440 | 159 | 8.4 | 1, 2, 3 | 1.4, 2.8, 4.3 | 48[f], 60[f], 72[f] | 48[f] |
| Xenon | 1,000[a] | 987 | 690 | 6,160 | 137 | 4.4, 8.8, 13.3 | 4, 8, 12 | 48, 60, 72, 84 | 48, 60, 72 |
| Chromium | 11.4[b] | 4.1 | 3,160 | 0.55 | 0.07 | 5, 20, 61 | 1, 4, 12 | 48, 60[e], 72, 84 | 48, 60[e], 72, 84 |
| Extended Bragg peak | | | | | | | | | |
| Carbon | 114–158[a] | | 60–85 | | | 0.5, 1, 2 | | 48[g], 60[g], 72[g], 84[g] | 48[g], 60, 72 |

[a–c] Particle exposure was performed at SIS[a], UNILAC[b] at GSI, or HIMAC[c] at NIRS

[d] Data subsets have been published in Ritter et al. (2002), Nasonova and Ritter (2004) and Lee et al. (2005)

[e] Data from Lee et al. (2005)

[f] Data from Ritter et al. (2002)

[g] A data subset has been published in Nasonova and Ritter (2004)

$E_{prim}$ is the primary energy of the particles delivered by the accelerator

$E$ is the average energy in the sample, and LET is the corresponding LET value

$R_{max}$ is the maximum radial range of energy deposition within a particle track

Range is the residual range of particles in water

dose and accelerator conditions, and the dose rate was in the range of several Gy/min. Accordingly, X-ray exposures were done with a dose rate of about 2 Gy/min. The beam characteristics, such as the ion type, the primary energy, the energy and LET on target (corrected for material in the beam path), and the residual range in water are given in Table 1.

For the exposure to monoenergetic charged particles with an energy ≥100 MeV/u, the cell suspension was loaded into specially designed polyethylene holders with a 2-mm-thick well for the sample and 1-mm plastic between the cells and the radiation source. Under this exposure condition, the contamination by lighter fragments was 2% or less, and their contribution to dose was less than 1%. The variation of LET in the sample was less than 5% for the lowest energy and decreased with increasing energy. Irradiation with a 25-mm extended Bragg peak, obtained by active energy variation of the beam in the range of 114–158 MeV/u, was performed in 5-ml plastic tubes (inside diameter 10 mm). Tubes were set in the middle of a 25-mm extended peak, which was designed to deliver an isodose distribution. Accordingly, in Table 1 the dose-averaged LET at the proximal and distal part of the sample is given (for further details see Nasonova and Ritter 2004). For the exposure to 11.4 MeV/u C-ions and Cr-ions with a short residual range (see Table 1), 10 μl of cell suspension was sandwiched between a polycarbonate foil (thickness: 14 μm, diameter: 29 mm) and a 35-mm Petri dish to have a liquid layer thickness of about 15 μm (Lee et al. 2005). X-ray irradiation was done in 25-cm$^2$ culture flasks or in polyethylene holders as described earlier.

Immediately after irradiation, cells were resuspended at a concentration of 0.5 × $10^6$ cells/ml in complete medium supplemented with 1% phytohemagglutinin (PHA; Invitrogen, Paisley, UK) and 5–15 μg/ml 5-bromo-2-deoxyuridine (BrdU; Serva, Heidelberg, Germany). All procedures from the addition of BrdU up to the fixation of cells were performed under subdued light to avoid photolysis of BrdU.

## Cytogenetic analysis

Chromosome aberrations were analyzed in metaphases and prematurely condensed $G_2$-phase cells collected at 48, 60, 72, and 84 h after radiation exposure. For metaphase analysis, colcemid (200 ng/ml, Roche, Mannheim, Germany) was added to the samples 3 h before harvest. Chromosome spreads were prepared according to standard techniques (IAEA 2001) and stained with the fluorescence-plus-Giemsa (FPG) technique (see Ritter et al. 1996) in

order to differentiate between cells in the first or a later cell generation. At each dose- and time-point, 100–300 first-cycle metaphases were scored based on the classification criteria by Savage (1976). All aberration types detectable by solid staining were scored, i.e., dicentric, centric and acentric rings, interstitial deletions, chromosome- and chromatid-type breaks, and chromatid-type exchanges. Chromatid-type aberrations were included in the analysis, because the induction of chromatid-type aberrations in $G_0/G_1$-cells is a specific feature of high-LET exposure as described in detail elsewhere (Ritter et al. 1996; Lee et al. 2005). About 80% of the chromatid-type aberrations found after high-LET exposure were chromatid-type breaks, while the remaining 20% were chromatid-type exchanges (i.e., mainly chromatid-type chromosome interchanges).

In the case of centric rings or dicentric chromosomes, one acentric fragment was assigned to each exchange. Polycentric chromosomes with n centromeres were counted as n−1 dicentric chromosomes. For a direct comparison with the data obtained for $G_2$-phase cells, the number of aberrations that result in an excess of chromosome fragments (i.e., terminal and interstitial deletions and acentric and centric rings) was determined.

For aberration analysis in $G_2$-phase cells, premature chromosome condensation (PCC) was chemically induced by adding 50 nM calyculin A (Alomone labs, Jerusalem, Israel) for 45 min (Lee et al. 2005; Gotoh and Durante 2006). PCC spreads were prepared and stained with FPG technique as described previously. At each dose- and time-point aberrations were measured in 100–200 first-cycle $G_2$-PCC cells that were differentiated from metaphases by chromosome structure. Both, $G_2$-cells and metaphase cells display fully condensed bivalent chromatids, but $G_2$-cells lack a visible centromere as shown in Nasonova and Ritter (2004). Therefore, only aberrations resulting in an excess of chromosome fragments have been scored, while dicentrics remain undetectable. Some subsets of the metaphase and PCC data have been previously published as indicated in Table 1.

### Error calculation and curve fitting

Aberration yields were averaged, and standard deviations were calculated from 3 experiments for X-rays and 2 experiments for each 400 MeV/u C-ions or extended Bragg peak C-ions. In case of single experiments, we assumed Poisson standard errors for the data points as it is normally done in radiation cytogenetics, although it should be pointed that this errors underestimate the uncertainty for broad overdispersed distributions. We did not use these uncertainties for any statistical testing. The errors should be interpreted as a broad indication of the statistical variance.

Least-squares fit of a linear-quadratic equation to data was performed using the statistical program (gd) available for UNIX workstations at GSI:

$$y = \alpha D + \beta D^2$$

where y is the aberration yield after subtracting the background level, $\alpha$ is the linear coefficient, and $\beta$ is the dose ($D$) squared coefficient. Errors of $\alpha$ and $\beta$ values were obtained from the confidence limits of the fit curve at one standard deviation.

## Results and discussion

### Analysis of aberrations in metaphase cells and $G_2$-PCC: impact of sampling time and LET

In the present study, we performed a systematic analysis of the time-course of chromosome aberrations induced in human lymphocytes by charged particles with differing LET or X-rays (see Table 1). In the first series of experiments, aberrations were measured in first-cycle metaphases collected at the standard sampling time of 48 h and at later times (i.e., 60, 72, and 84 h). Selected dose–response curves for total chromosome aberration yields are shown in Fig. 1. Following the exposure to X-rays (Fig. 1a) or low-LET particles such as 11 and 14 keV/$\mu$ C-ions (not shown), the dose–response was linear-quadratic. In contrast, when lymphocytes were exposed to particles with higher LET values, the dose–response curves were either linear for particles with an energy >90 MeV/u (see Fig. 1b, c, e–g) or saturated for particles with an energy <10 MeV/u (Fig. 1d, h).

For X-rays and particles with LET values up to 29 keV/μm, no or only minor changes in the aberration frequencies with time occurred consistent with previous reports on the effects of $\gamma$-rays, X-rays, or 30 keV/μm Ne-ions (George et al. 2001; Ritter et al. 2002; Hoffmann et al. 2002; Lee et al. 2005; Heimers et al. 2005). In contrast, for heavy ions with higher LET values, a marked rise in the aberration yield with culture time was found, i.e., cells that entered the first mitosis at 84 h carried up to 20 times more aberrations than those arriving at 48 h (Fig. 1c–h). The same trend was observed when we restricted the analysis to aberration subclasses such as dicentrics or excess acentric fragments (data not shown). Likewise, a marked increase in the aberration yield with time was observed in the few studies applying fluorescence in situ hybridization technique (FISH) for the detection of cytogenetic damages induced by charged particles with LET values of 121, 140, and 175 keV/μm, respectively (Anderson et al. 2000; George et al. 2001; Lee et al. 2010). Altogether, these data clearly demonstrate that the analysis of radiation-induced aberrations in metaphase cells at a single early harvesting

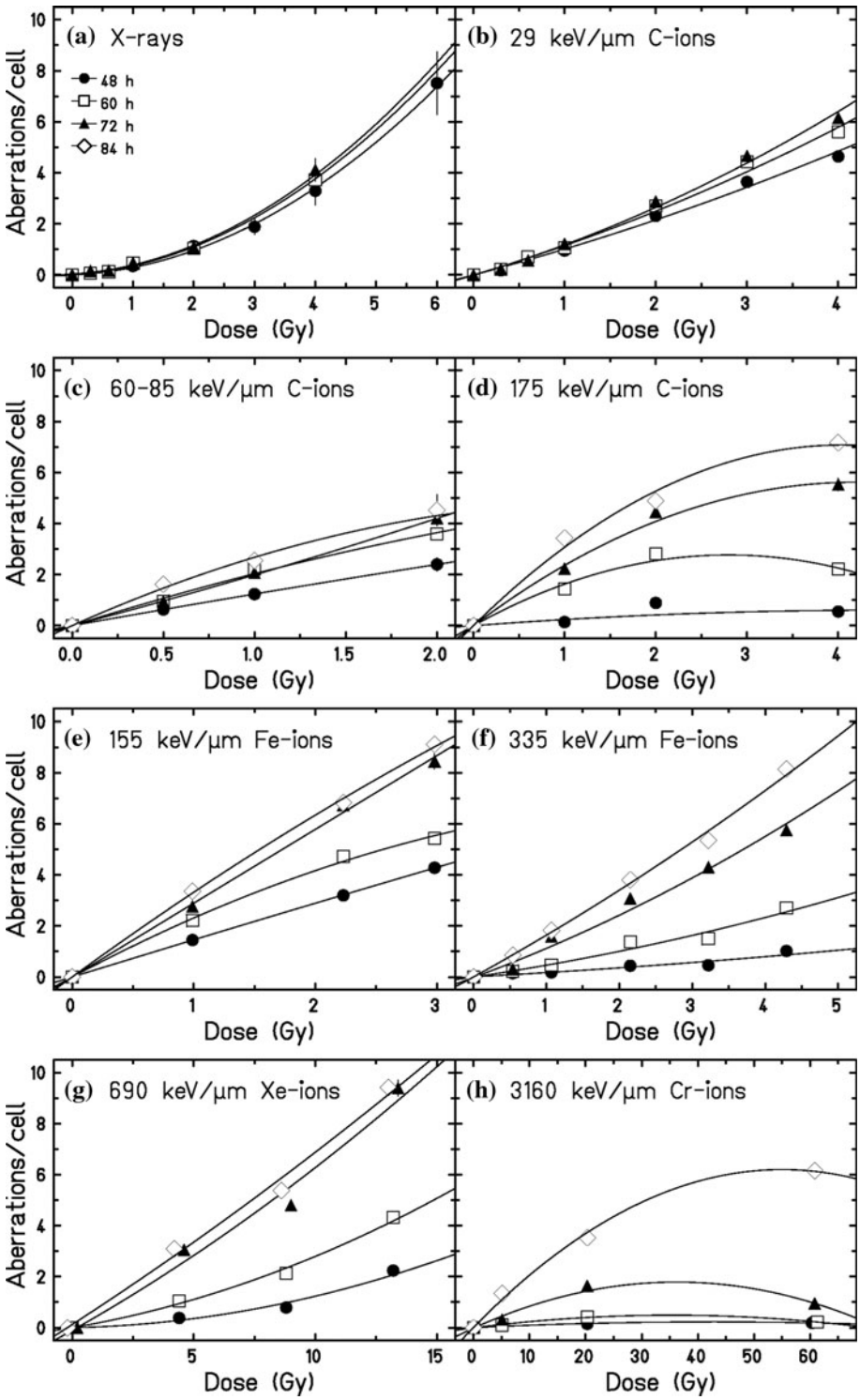


**Fig. 1** Dose–response curves of the yields of total chromosome aberration in first-cycle metaphases. Human lymphocytes were collected at 48–84 h after exposure to X-rays or heavy ions: **a** X-rays, **b** 90 MeV/u C-ions (LET = 29 keV/μm), **c** extended Bragg peak C-ions (60–85 keV/μm), **d** 9.5 MeV/u C-ions (175 keV/μm), **e** 990 MeV/u Fe-ions (155 keV/μm), **f** 177 MeV/u Fe-ions (335 keV/μm), **g** 987 MeV/u Xe-ions (690 keV/μm), and **h** 4.1 MeV/u Cr-ions (3,160 keV/μm). Background values were subtracted, and linear-quadratic equations were fit to the data. Note different x-axes scaling

time as recommended by IAEA (2001) can lead to a severe underestimation of the effectiveness of densely ionizing particles.

To assess whether the $G_2$-PCC assay at 48 h postirradiation accounts for heavy-ion-induced cell cycle delay of damaged cells, aberrations were measured at 48 h and compared to that obtained at later sampling times (see Table 1). Preliminary analysis of cell populations prematurely condensed by calyculin A showed that the percentage of lymphocytes arrested at the first $G_2$-phase depends on LET and dose. For example, while most nonirradiated lymphocytes completed the first cell cycle by 72 h and less than 5% of the population were in the first $G_2$-phase, after exposure to 1 Gy of X-rays or 175 keV/μm C-ions, the

proportion of first-$G_2$-phase lymphocytes amounted to 9 and 31%, respectively. After exposure to 4 Gy X-rays or C-ions, these proportions rose to 30 and 55% (data not shown).

As mentioned in the introduction, in most studies performed up to now, PCC cells were harvested at 48 h as initially suggested (Durante et al. 1998; Kanda et al. 1999), and we are only aware of one study, where two sampling times were used. George et al. (2001) scored aberrations in $G_2$/M lymphocytes collected at 48 h and at 72 h after irradiation with 1 GeV/u Fe-ions (LET = 140 keV/μm) and found similar aberration yields at both times. However, in this study, the differentiation of cell generations failed. Thus, the aberration yield measured in cells harvested at 72 h is probably underestimated, because cells at later cell divisions that carry fewer aberrations than first-cycle cells (e.g., Sasaki and Norman 1967; Bauchinger et al. 1986; Krishnaja and Sharma 2004) have been included in the analysis.

Our experiments revealed that in $G_2$-PCC cells like in metaphases, the level of aberrations is stable or changes only minimal with time after exposure to X-rays or low-LET particles, but increases when high-LET particles are applied (Fig. 2). However, this effect was less pronounced in PCC samples compared to metaphase samples (compare Figs. 1, 2), demonstrating for the first time that the proposed $G_2$-PCC assay at 48 h postirradiation accounts for most, but not all, of high-LET-induced cell cycle delay of severely damaged lymphocytes.

## Fitting of the dose–effect curves

To facilitate a more detailed comparison of the impact of sampling time and LET on the measured aberration yields in first-cycle metaphases or $G_2$-PCC cells, linear-quadratic equations were fitted to the data and the fit parameters $\alpha$ and $\beta$ were derived. Table 2 shows the fit parameters obtained from the total aberration yields in metaphase cells and from the number of excess fragments measured in metaphase and $G_2$-PCC cells, respectively. The resulting $\alpha$ values and those derived from the yields of dicentric chromosomes in metaphases are plotted in Fig. 3. For the quadratic component $\beta$, larger values were obtained after X-irradiation and the $\beta$ values were smaller following exposure to particles in both metaphases and $G_2$-PCC. Negative $\beta$ values were mainly derived from data sets for low-energy particles such as 9.5 MeV/u C-ions (LET = 175 keV/μm) or 4.1 MeV/u Cr-ions (LET = 3,160 keV/μm) due to the saturation in the aberration yield (see Table 2). The curves should then be intended as a guide for the trend of the data points. Some $\alpha$ values are also very small (e.g., for X-rays), but we have not refitted the data excluding the $\alpha$ parameter, because we are assuming the linear-quadratic model for describing the aberration yields. Data in Fig. 3 can therefore be interpreted as a trend for the aberration frequency at low doses. For a more precise estimate of the fit parameters $\alpha$ and $\beta$, repeated experiments with a larger number of dose-points have to be performed.

Analysis of the dose–response curves for total aberrations, dicentrics, or excess fragments expressed in metaphase cells at 48 h postirradiation showed that the $\alpha$ values increased with LET, reached a maximum around 155 keV/μm, and decreased steeply with a further rise in LET (Fig. 3a–c; Table 2). George et al. (2003) reported a similar LET dependence of $\alpha$ values for simple and complex exchanges in human lymphocytes collected in metaphase 48 h after exposure. Analysis of the dose–response curves generated at later sampling times showed that the fit parameter $\alpha$ is clearly time dependent for particles with LET > 30 keV/μm, i.e., $\alpha$ values derived from metaphases collected at later times were higher than those obtained for cells harvested at 48 h (Fig. 3a–c; Table 2).

Accordingly, the dose–response data for $G_2$-PCC (Fig. 2) were analyzed. As observed for metaphase cells, the $\alpha$ values derived from PCC samples increased with LET and peaked around 155 keV/μm (Fig. 3d). However, in contrast to metaphase analysis, the $\alpha$ coefficients from PCC samples declined less steeply and, as expected from Figs. 1, 2, the time-dependent changes in the parameter $\alpha$ were smaller for $G_2$-PCC analysis than for metaphase analysis.

To gain further insights into how cell cycle delays affect the aberration yield observable in $G_2$-phase or metaphase, we compared the $\alpha$ values derived for excess acentric fragments, the aberration class detectable with both assays. At any sampling time, higher $\alpha$ values were obtained from PCC samples (Fig. 3d) than from metaphases (Fig. 3c), confirming that many damaged lymphocytes undergo a severe $G_2$-block that prevents their entry into mitosis (e.g., Durante et al. 1999; George et al. 2003). The largest differences were observed at 48 h after exposure to C-ions with LET = 175 keV/μm and at any investigated time-point after exposure to Fe-, Xe-, or Cr-ions with LET values ≥335 keV/μm (see Table 2; Fig. 3c, d). The latter observation suggests that high-LET radiation induces not only a transient but also a sustained arrest of heavily damaged lymphocytes in $G_2$. Whether cells suffering a prolonged $G_2$-arrest will ever progress to the first postirradiation mitosis remains to be determined. Certainly, the number of aberrations detectable in $G_2$ or metaphase is also affected by apoptosis. In preceding studies, we observed a low-apoptotic rate in human lymphocytes after exposure to X-rays or Fe-ions with 155 and 335 keV/μm, but a high rate (up to 40%) after exposure to Cr-ions with 3,160 keV/μm (Lee et al. 2005).

## Impact of the microscopic dose distribution on the aberration yield

The observed differences in the time-course of aberrations observed after low- and high-LET radiation (Figs. 1, 2) are

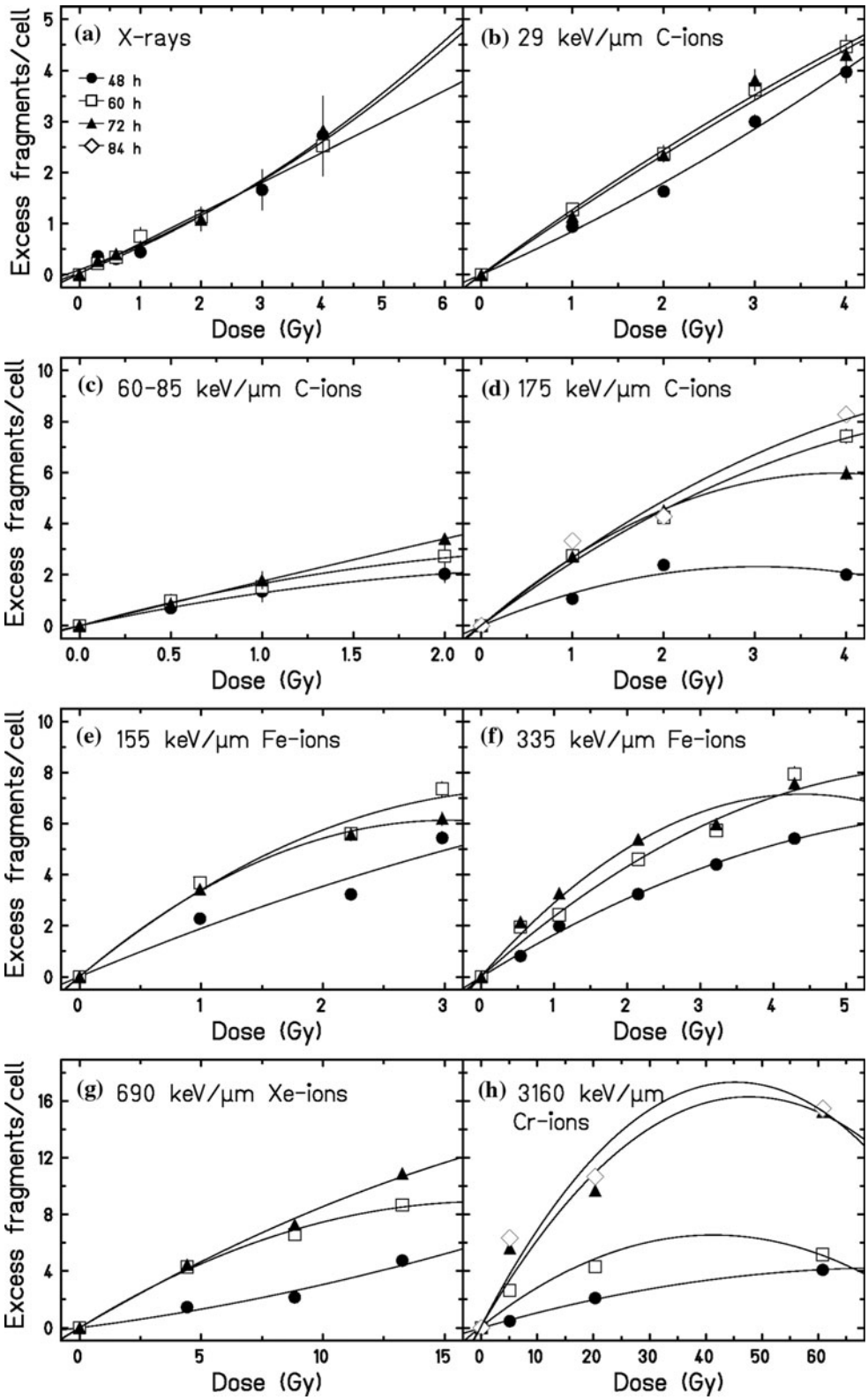


**Fig. 2** Dose–response curves of the yields of aberrations detectable in first-cycle $G_2$-PCC cells. Because of the morphology of $G_2$-PCC, only aberrations resulting in an excess of chromosome fragments (i.e., terminal and interstitial deletions, acentric and centric rings) are detectable. Human lymphocytes were collected at 48–84 h postirradiation following a treatment with calyculin A to induce PCC in interphase cells. Background values were subtracted, and linear-quadratic equations were fit to the data. Note different x- and y-axes scaling

attributable to the difference in the spatial energy deposition. For X-rays, the energy deposition on a micrometer scale, i.e., in the dimension of a cell nucleus, is uniform, leading to a homogeneous distribution of aberrations and delay times within the cell population. In contrast, charged particles distribute their energy inhomogeneously with two characteristics. The first is that the number of hits per nucleus is randomly distributed among the cells (e.g., see

**Table 2** Fit parameters obtained for linear-quadratic dose–effect curves of total aberrations in first-cycle metaphases and excess fragments in first-cycle $G_2$-PCC cells collected at 48–84 h postirradiation

| Radiation type | LET (keV/μm) | Fix time (h) | Metaphases (total aberrations) | | Metaphases (excess fragments) | | $G_2$-PCC (excess fragments) | |
|---|---|---|---|---|---|---|---|---|
| | | | $\alpha \pm$ SE ($Gy^{-1}$) | $\beta \pm$ SE ($Gy^{-2}$) | $\alpha \pm$ SE ($Gy^{-1}$) | $\beta \pm$ SE ($Gy^{-2}$) | $\alpha \pm$ SE ($Gy^{-1}$) | $\beta \pm$ SE ($Gy^{-2}$) |
| X-rays | 2 | 48 | 0.10 ± 0.06 | 0.19 ± 0.03 | 0.10 ± 0.04 | 0.068 ± 0.017 | 0.46 ± 0.10 | 0.05 ± 0.03 |
| | | 60 | 0.16 ± 0.06 | 0.20 ± 0.02 | 0.070 ± 0.048 | 0.085 ± 0.023 | 0.59 ± 0.17 | 0.001 ± 0.06 |
| | | 72 | 0.15 ± 0.07 | 0.20 ± 0.03 | 0.062 ± 0.052 | 0.096 ± 0.016 | 0.44 ± 0.19 | 0.05 ± 0.07 |
| Carbon | 11 | 48 | 0.33 ± 0.08 | 0.15 ± 0.04 | 0.21 ± 0.06 | 0.056 ± 0.019 | n.d. | |
| Carbon | 14 | 48 | 0.52 ± 0.07 | 0.10 ± 0.02 | 0.22 ± 0.05 | 0.042 ± 0.016 | n.d. | |
| | | 72 | 0.58 ± 0.08 | 0.11 ± 0.03 | 0.21 ± 0.05 | 0.071 ± 0.017 | n.d. | |
| Carbon | 29 | 48 | 0.95 ± 0.07 | 0.07 ± 0.02 | 0.38 ± 0.05 | 0.041 ± 0.015 | 0.8 ± 0.1 | 0.05 ± 0.03 |
| | | 60 | 1.1 ± 0.1 | 0.10 ± 0.03 | 0.49 ± 0.06 | 0.029 ± 0.017 | 1.3 ± 0.1 | −0.05 ± 0.03 |
| | | 72 | 1.1 ± 0.1 | 0.14 ± 0.03 | 0.48 ± 0.06 | 0.075 ± 0.019 | 1.3 ± 0.1 | −0.04 ± 0.03 |
| Carbon extended Bragg peak | 60–85 | 48 | 1.3 ± 0.2 | −0.04 ± 0.12 | 0.64 ± 0.13 | −0.049 ± 0.077 | 1.6 ± 0.4 | −0.3 ± 0.2 |
| | | 60 | 2.3 ± 0.2 | −0.22 ± 0.13 | 1.2 ± 0.2 | −0.21 ± 0.09 | 2.0 ± 0.5 | −0.3 ± 0.4 |
| | | 72 | 1.9 ± 0.2 | 0.11 ± 0.12 | 0.77 ± 0.23 | 0.15 ± 0.14 | 1.8 ± 0.5 | −0.04 ± 0.2 |
| | | 84 | 3.2 ± 0.4 | −0.52 ± 0.29 | 1.4 ± 0.3 | −0.20 ± 0.26 | n.d. | |
| Carbon | 175 | 48 | 0.3 ± 0.2 | −0.03 ± 0.05 | 0.10 ± 0.03 | −0.0065 ± 0.0094 | 1.5 ± 0.1 | −0.25 ± 0.03 |
| | | 60 | 2.0 ± 0.1 | −0.35 ± 0.03 | 0.88 ± 0.08 | −0.14 ± 0.02 | 2.7 ± 0.2 | −0.21 ± 0.05 |
| | | 72 | 2.7 ± 0.1 | −0.32 ± 0.04 | 1.3 ± 0.1 | −0.13 ± 0.03 | 3.1 ± 0.2 | −0.39 ± 0.05 |
| | | 84 | 3.5 ± 0.2 | −0.43 ± 0.05 | 1.7 ± 0.1 | −0.14 ± 0.04 | 2.9 ± 0.2 | −0.21 ± 0.05 |
| Iron | 155 | 48 | 1.5 ± 0.2 | −0.01 ± 0.07 | 0.64 ± 0.12 | 0.042 ± 0.049 | 2.0 ± 0.2 | −0.12 ± 0.09 |
| | | 60 | 2.5 ± 0.2 | −0.23 ± 0.08 | 1.3 ± 0.2 | −0.091 ± 0.062 | 3.9 ± 0.3 | −0.52 ± 0.11 |
| | | 72 | 2.9 ± 0.2 | −0.0002 ± 0.10 | 1.2 ± 0.2 | 0.15 ± 0.07 | 4.0 ± 0.3 | −0.67 ± 0.10 |
| | | 84 | 3.5 ± 0.3 | −0.15 ± 0.10 | 1.9 ± 0.2 | −0.055 ± 0.078 | n.d. | |
| Iron | 335 | 48 | 0.15 ± 0.04 | 0.01 ± 0.01 | 0.10 ± 0.03 | 0.0011 ± 0.0093 | 1.8 ± 0.1 | −0.12 ± 0.03 |
| | | 60 | 0.4 ± 0.1 | 0.04 ± 0.02 | 0.24 ± 0.05 | 0.026 ± 0.015 | 2.5 ± 0.1 | −0.20 ± 0.04 |
| | | 72 | 1.1 ± 0.1 | 0.08 ± 0.03 | 0.55 ± 0.07 | 0.056 ± 0.020 | 3.2 ± 0.1 | −0.37 ± 0.03 |
| | | 84 | 1.6 ± 0.1 | 0.06 ± 0.04 | 1.0 ± 0.1 | 0.016 ± 0.027 | n.d. | |
| Iron | 440 | 48 | 0.03 ± 0.05 | 0.026 ± 0.018 | 0.003 ± 0.029 | 0.014 ± 0.011 | 1.4 ± 0.2 | −0.18 ± 0.06 |
| | | 60 | 0.82 ± 0.11 | −0.064 ± 0.045 | 0.50 ± 0.09 | −0.042 ± 0.034 | n.d. | |
| Xenon | 690 | 48 | 0.02 ± 0.02 | 0.010 ± 0.002 | −0.001 ± 0.014 | 0.0054 ± 0.0014 | 0.22 ± 0.04 | 0.009 ± 0.003 |
| | | 60 | 0.16 ± 0.03 | 0.012 ± 0.003 | 0.096 ± 0.025 | 0.0062 ± 0.0023 | 1.1 ± 0.1 | −0.032 ± 0.005 |
| | | 72 | 0.54 ± 0.05 | 0.010 ± 0.005 | 0.28 ± 0.04 | 0.0077 ± 0.0036 | 1.0 ± 0.1 | −0.016 ± 0.006 |
| | | 84 | 0.61 ± 0.05 | 0.006 ± 0.005 | 0.40 ± 0.04 | −0.0009 ± 0.0038 | n.d. | |
| Chromium | 3,160 | 48 | 0.010 ± 0.003 | −0.0001 ± 0.0001 | 0.0034 ± 0.0022 | −0.00002 ± 0.00004 | 0.11 ± 0.01 | −0.0008 ± 0.0002 |
| | | 60 | 0.028 ± 0.005 | −0.0004 ± 0.0001 | 0.012 ± 0.003 | −0.00016 ± 0.00005 | 0.31 ± 0.02 | −0.0038 ± 0.0003 |
| | | 72 | 0.10 ± 0.01 | −0.0014 ± 0.0001 | 0.058 ± 0.006 | −0.00077 ± 0.00010 | 0.68 ± 0.02 | −0.0071 ± 0.0004 |
| | | 84 | 0.23 ± 0.01 | −0.0020 ± 0.0002 | 0.13 ± 0.01 | −0.0012 ± 0.0002 | 0.76 ± 0.02 | −0.0084 ± 0.0004 |

Virsik and Harder 1981). For human lymphocytes with a nuclear cross-sectional area of about 25 $\mu m^2$ (Anderson et al. 2000), a particle fluence of $4 \times 10^6$ particles/$cm^2$ leads to a mean number of one direct particle hit per cell nucleus. According to Poisson statistics, 37% of the nuclei receive no direct hit, while 37% are hit once, 18% are hit twice, and 8% are hit by ≥3 particles. The second feature is that the energy deposition of charged particles is highly localized along the particle trajectory as reviewed by Scholz (2003). The average energy deposition at a distance r from the trajectory obeys a $1/r^2$ law, and the maximum radial range follows a power law of the energy of the ion (Kiefer and Straaten 1986). Hence, the inhomogeneous dose deposition of particles results in a quite different distribution of aberrations among cells (Virsik and Harder 1981; Gudowska-Nowak et al. 2007; Deperas-Standylo et al. 2010) and subsequently in quite different delay times as reflected in Fig. 1d–h.

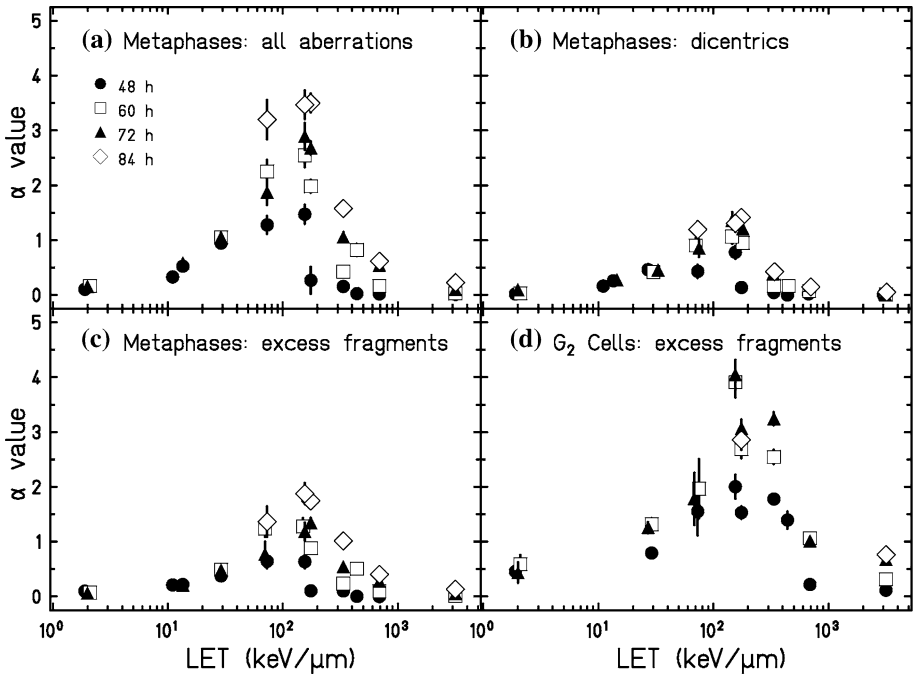


**Fig. 3** LET and time dependence of the linear coefficients α derived from the dose–response curves for the induction of aberrations in metaphase or $G_2$-PCC cells. In metaphase cells, the yields of total chromosome aberrations (**a**), dicentrics (**b**), and excess fragments (**c**) were analyzed. In $G_2$-PCC cells, the analysis was restricted to excess fragments (**d**) due to technical reasons

The impact of the track structure of particles on the time-course of aberrations is clearly visible, when the aberration yields produced by charged particles with a similar LET but a different energy and consequently a different track radius are compared, i.e., 175 keV/μm C-ions with 9.5 MeV/u ($R_{max}$ = 2.3 μm) and 155 keV/μm Fe-ions with 990 MeV/u ($R_{max}$ = 6,200 μm), respectively. As shown in Fig. 1, at 48 h postirradiation, the aberration frequencies were higher in lymphocytes exposed to Fe-ions (Fig. 1e) than in cells irradiated with C-ions (Fig. 1d). At the subsequent sampling times, the aberration yield increased about twice after Fe-ion exposure, while after C-ion exposure, an up to 24-fold rise was found.

The cytogenetic response to low-energy C-ions is attributable to the fact that their track radius is smaller than the radius of the cell nucleus of lymphocytes. For the applied fluences (see Table 1), a fraction of lymphocytes is not hit at all and will progress unperturbed through the cell cycle, while cells receiving one or more particle hits to the nucleus will suffer modest to severe damage and subsequently are delayed in the cell cycle progression. In contrast, in the case of high-energy Fe-ions, the track radius is much larger than the radius of the cell nucleus. Thus, the energy deposition of one particle is not restricted to the cell nucleus it actually traverses, but affects also neighboring cells. For high particle fluence, the particle tracks start to overlap, leading to a more homogeneous dose distribution compared to low-energy ions as described in more detail elsewhere (Scholz 2003). As a consequence, high-energy Fe-ions produce aberrations even in cells receiving no direct hit, reducing the difference in aberration yields between cells reaching mitosis at earlier or later times. More detailed statistical analyses or modeling studies that have been recently started (Gudowska-Nowak et al. 2007; Deperas-Standylo et al. 2010) will provide further insights into the interrelation of the number of aberrations carried by a cell, the cell cycle progression delay, and the particle track structure.

## Particle fluence response of aberration yields in metaphases and $G_2$-PCC cells

To allow a comparison of the cytogenetic effects of the applied ion beams on the basis of particle traversals per cell nucleus, the aberration yields analyzed in both metaphases and $G_2$-PCC cells collected at 48 and 72 h were plotted versus particle fluence. As mentioned earlier, a fluence of 4 x $10^6$ particles/cm$^2$ leads to an average of one traversal per cell nucleus for lymphocytes. As shown in Fig. 4a, in metaphases collected at 48 h, a mean number of one particle traversal per nucleus resulted in similar aberration yields for most ions; only 155 keV/μm Fe-ions were considerably more efficient. At 72 h, higher aberration frequencies were observed for particles with LET > 30 keV/μm (Fig. 4c), reflecting the specific LET- and time-dependent changes in the aberration yield (Figs. 1, 3a–c).

The fluence–effect curves obtained for $G_2$-PCC revealed a different picture (Fig. 4b, d). For $G_2$-cells, the differences in the effectiveness of the ions studied were more pronounced than for metaphases. Furthermore, $G_2$-PCC harvested at 48 h after exposure to 335 and 440 keV/μm Fe-ions displayed the highest aberration yield, i.e., a mean

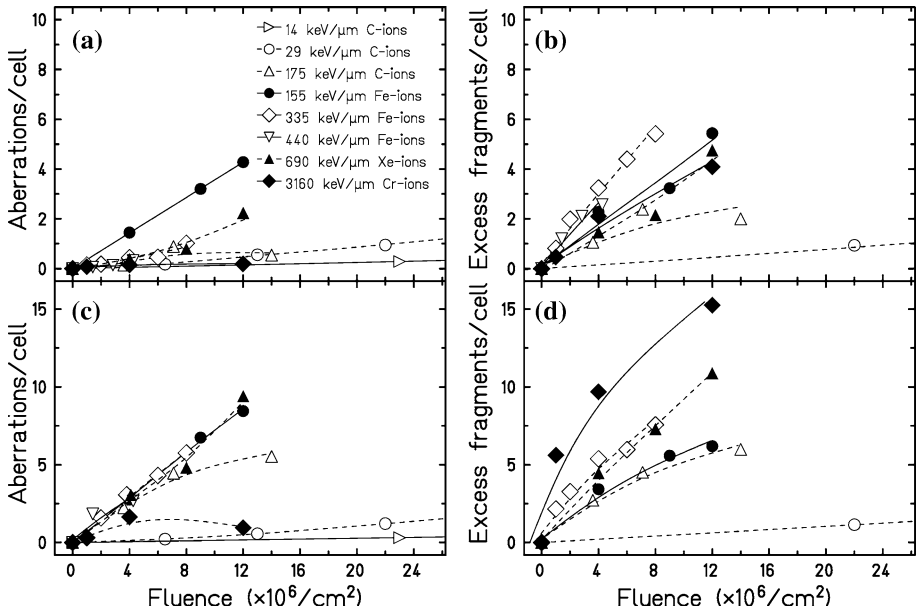


**Fig. 4** Total chromosome aberration yield in first-cycle metaphases (**a** and **c**) and yield of excess fragments in first-cycle $G_2$-PCC cells (**b** and **d**) as a function of particle fluence (data are replotted from Figs. 1 and 2). Samples were harvested at 48 h (**a** and **b**) or 72 h (**c** and **d**) postirradiation. *Lines* are drawn to guide the eye. A particle fluence of 4 x $10^6$ ions/$cm^2$ corresponds to a mean number of one direct hit per nucleus for human lymphocytes

number of one particle traversal through a cell nucleus induced about 3 excess fragments (Fig. 4b). At the later time, 3,160 keV/µm Cr-ions were found to be most effective producing about 10 excess fragments per hit (Fig. 4d). Altogether, the experimental data prove that the $G_2$-PCC assay is more suitable than the metaphase assay for detecting extensive high-LET-induced cytogenetic damage. Yet, if cells are traversed by particles with a very high LET, still a fraction of heavily damaged and drastically delayed cells is not included in the analysis when $G_2$-PCC are harvested only at 48 h postirradiation. Thus, in case of a suspected exposure to particles with a very high LET, aberrations should also be measured at a second (later) sampling time even if the $G_2$-PCC assay is applied.

**Acknowledgments** We acknowledge P. Hessel for skillful assistance in cell culture, Dr M. Scholz and Dr T. Elsässer for planning and realizing the particle exposure of cells, W. Becher and G. Lenz for technical assistance during particle irradiation, and Prof Dr G. Kraft and Prof Dr E. Gudowska-Nowak for fruitful discussions. This work was supported by the Federal Ministry of Education and Research (Bonn, Germany under contract number 02S8203 and 02S8497) and by the European Space Agency (ESA-IBER project: Investigations into Biological Effects of Radiation).

## References

Anderson RM, Marsden SJ, Wright EG, Kadhim MA, Goodhead DT, Griffin CS (2000) Complex chromosome aberrations in peripheral blood lymphocytes as a potential biomarker of exposure to high-LET alpha-particles. Int J Radiat Biol 76:31–42

Bauchinger M, Schmid E (1998) LET dependence of yield ratios of radiation-induced intra- and interchromosomal aberrations in human lymphocytes. Int J Radiat Biol 74:17–25

Bauchinger M, Schmid E, Braselmann H (1986) Cell survival and radiation induced chromosome aberrations. II. Experimental findings in human lymphocytes analysed in first and second post-irradiation metaphases. Radiat Environ Biophys 25:253–260

Bonassi S, Norppa H, Ceppi M, Stromberg U, Vermeulen R, Znaor A, Cebulska-Wasilewska A, Fabianova E, Fucic A, Gundy S, Hansteen IL, Knudsen LE, Lazutka J, Rossner P, Sram RJ, Boffetta P (2008) Chromosomal aberration frequency in lymphocytes predicts the risk of cancer: results from a pooled cohort study of 22 358 subjects in 11 countries. Carcinogenesis 29:1178–1183

Combs SE, Nikoghosyan A, Jaekel O, Karger CP, Haberer T, Munter MW, Huber PE, Debus J, Schulz-Ertner D (2009) Carbon ion radiotherapy for pediatric patients and young adults treated for tumors of the skull base. Cancer 115:1348–1355

Cucinotta FA, Durante M (2006) Cancer risk from exposure to galactic cosmic rays: implications for space exploration by human beings. Lancet Oncol 7:431–435

Deperas-Standylo J, Lee R, Ayriyan A, Nasonova E, Ritter S, Gudowska-Nowak E (2010) Time-course of aberrations and their distribution: impact of LET and track structure. Eur Phys J D 60:93–99

Dickerman JD (2007) The late effects of childhood cancer therapy. Pediatrics 119:554–568

Durante M, Cucinotta FA (2008) Heavy ion carcinogenesis and human space exploration. Nat Rev Cancer 8:465–472

Durante M, Loeffler JS (2010) Charged particles in radiation oncology. Nat Rev Clin Oncol 7:37–43

Durante M, George K, Yang TC (1997) Biodosimetry of ionizing radiation by selective painting of prematurely condensed chromosomes in human lymphocytes. Radiat Res 148:S45–S50

Durante M, Furusawa Y, Gotoh E (1998) A simple method for simultaneous interphase-metaphase chromosome analysis in biodosimetry. Int J Radiat Biol 74:457–462

Durante M, Furusawa Y, Majima H, Kawata T, Gotoh E (1999) Association between G2-phase block and repair of radiation-induced chromosome fragments in human lymphocytes. Radiat Res 151:670–676

Fokas E, Kraft G, An H, Engenhart-Cabillic R (2009) Ion beam radiobiology and cancer: time to update ourselves. Biochim Biophys Acta 1796:216–229

George K, Wu H, Willingham V, Furusawa Y, Kawata T, Cucinotta FA (2001) High- and low-LET induced chromosome damage in

human lymphocytes: a time-course of aberrations in metaphase and interphase. Int J Radiat Biol 77:175–183
George K, Durante M, Willingham V, Wu H, Yang TC, Cucinotta FA (2003) Biological effectiveness of accelerated particles for the induction of chromosome damage measured in metaphase and interphase human lymphocytes. Radiat Res 160:425–435
Gotoh E, Durante M (2006) Chromosome condensation outside of mitosis: mechanisms and new tools. J Cell Physiol 209:297–304
Gotoh E, Tanno Y (2005) Simple biodosimetry method for cases of high-dose radiation exposure using the ratio of the longest/shortest length of Giemsa-stained drug-induced prematurely condensed chromosomes (PCC). Int J Radiat Biol 81:379–385
Gudowska-Nowak E, Kleczkowski A, Nasonova E, Scholz M, Ritter S (2005) Correlation between mitotic delay and aberration burden, and their role for the analysis of chromosomal damage. Int J Radiat Biol 81:23–32
Gudowska-Nowak E, Lee R, Nasonova E, Ritter S, Scholz M (2007) Effect of LET and track structure on the statistical distribution of chromosome aberrations. Advances Space Res 39:1070–1075
Haberer T, Becher W, Schardt D, Kraft G (1993) Magnetic scanning system for heavy ion therapy. Nucl Instrum Methods Phys Res Sect A 330:296–305
Heimers A, Brede HJ, Giesen U, Hoffmann W (2005) Influence of mitotic delay on the results of biological dosimetry for high doses of ionizing radiation. Radiat Environ Biophys 44:211–218
Hoffmann GR, Sayer AM, Littlefield LG (2002) Higher frequency of chromosome aberrations in late-arising first-division metaphases than in early-arising metaphases after exposure of human lymphocytes to X-rays in G0. Int J Radiat Biol 78:765–772
IAEA (2001) Cytogenetic analysis for radiation dose assessment: a manual. Technical Reports Series 405
Kanda R, Hayata I, Lloyd DC (1999) Easy biodosimetry for high-dose radiation exposures using drug-induced, prematurely condensed chromosomes. Int J Radiat Biol 75:441–446
Kiefer J, Straaten H (1986) A model of ion track structure based on classical collision dynamics. Phys Med Biol 31:1201–1209
Kraft G, Daues HW, Fischer B, Kopf U, Leibold HB, Quis D, Stelzer H, Kiefer J, Schöpfer R, Schneider E, Weber U, Wulf H, Dertinger H (1980) Irradiation chamber and sample changes for biological samples. Nucl Instrum Meth 168:175–179
Krishnaja AP, Sharma NK (2004) Transmission of gamma-ray-induced unstable chromosomal aberrations through successive mitotic divisions in human lymphocytes in vitro. Mutagenesis 19:299–305
Lee R, Nasonova E, Ritter S (2005) Chromosome aberration yields and apoptosis in human lymphocytes irradiated with Fe-ions of differing LET. Adv Space Res 35:268–275
Lee R, Sommer S, Hartel C, Nasonova E, Durante M, Ritter S (2010) Complex exchanges are responsible for the increased effectiveness of C-ions compared to X-rays at the first post-irradiation mitosis. Mutat Res 701:52–59
Lindholm C, Salomaa S, Tekkel M, Paile W, Koivistoinen A, Ilus T, Veidebaum T (1996) Biodosimetry after accidental radiation exposure by conventional chromosome analysis and FISH. Int J Radiat Biol 70:647–656
Lucke-Huhle C, Blakely EA, Chang PY, Tobias CA (1979) Drastic G2 arrest in mammalian cells after irradiation with heavy-ion beams. Radiat Res 79:97–112
Merchant TE (2009) Proton beam therapy in pediatric oncology. Cancer J 15:298–305
Minohara S, Fukuda S, Kanematsu N, Takei Y, Furukawa T, Inaniwa T, Matsufuji N, Mori S, Noda K (2010) Recent innovations in carbon-ion radiotherapy. J Radiat Res (Tokyo) 51:385–392
Nasonova E, Ritter S (2004) Cytogenetic effects of densely ionising radiation in human lymphocytes: impact of cell cycle delays. Cytogenet Genome Res 104:216–220
Ochab-Marcinek A, Gudowska-Nowak E, Nasonova E, Ritter S (2009) Modeling radiation-induced cell cycle delays. Radiat Environ Biophys 48:361–370
Ritter S, Durante M (2010) Heavy-ion induced chromosomal aberrations: a review. Mutat Res 701:38–46
Ritter S, Nasonova E, Scholz M, Kraft-Weyrather W, Kraft G (1996) Comparison of chromosomal damage induced by X-rays and Ar ions with an LET of 1840 keV/micrometer in G1 V79 cells. Int J Radiat Biol 69:155–166
Ritter S, Nasonova E, Furusawa Y, Ando K (2002) Relationship between aberration yield and mitotic delay in human lymphocytes exposed to 200 MeV/u Fe-ions or X-rays. J Radiat Res (Tokyo) 43(Suppl):S175–S179
Sasaki MS, Norman A (1967) Selection against chromosome aberrations in human lymphocytes. Nature 214:502–503
Sasaki MS, Hayata I, Kamada N, Kodama Y, Kodama S (2001) Chromosome aberration analysis in persons exposed to low-level radiation from the JCO criticality accident in Tokai-mura. J Radiat Res (Tokyo) 42(Suppl):S107–S116
Savage JR (1976) Classification and relationships of induced chromosomal structural changes. J Med Genet 13:103–122
Scholz M (2003) Effects of ion radiation on cells and tissues. Advances Polym Sci 162:95–155
Scholz M, Kraft-Weyrather W, Ritter S, Kraft G (1994) Cell cycle delays induced by heavy ion irradiation of synchronous mammalian cells. Int J Radiat Biol 66:59–75
Scholz M, Ritter S, Kraft G (1998) Analysis of chromosome damage based on the time course of aberrations. Int J Radiat Biol 74:325–331
Schulz-Ertner D (2009) The clinical experience with particle therapy in adults. Cancer J 15:306–311
Suzuki M, Nakano K, Suzuki K, Watanabe M (2000) Influence of the sampling time on chromosomal aberrations at G2 phase in Syrian hamster embryonic cells irradiated with different types of radiation. Int J Radiat Biol 76:815–821
Testard I, Dutrillaux B, Sabatier L (1997) Chromosomal aberrations induced in human lymphocytes by high-LET irradiation. Int J Radiat Biol 72:423–433
Tsujii H, Kamada T, Baba M, Tsuji H, Kato H, Kato S, Yamada S, Yasuda S, Yanagi T, Kato H, Hara R, Yamamoto N, Mizoe J (2008) Clinical advantages of carbon-ion radiotherapy. New J Phys 10:075009
Virsik RP, Harder D (1981) Statistical interpretation of the overdispersed distribution of radiation-induced dicentric chromosome aberrations at high LET. Radiat Res 85:13–23
Wojcik A, Stephan G, Sommer S, Buraczewska I, Kuszewski T, Wieczorek A, Gozdz S (2003) Chromosomal aberrations and micronuclei in lymphocytes of breast cancer patients after an accident during radiotherapy with 8 MeV electrons. Radiat Res 160:677–683